



MOX-Report No. 33/2016

**hp-version discontinuous Galerkin approximations of
the elastodynamics equation**

Antonietti, P. F.; Ferroni, A.; Mazzieri, I.; Quarteroni, A.

MOX, Dipartimento di Matematica
Politecnico di Milano, Via Bonardi 9 - 20133 Milano (Italy)

mox-dmat@polimi.it

<http://mox.polimi.it>

hp–version discontinuous Galerkin approximations of the elastodynamics equation*

Paola F. Antonietti[‡], Alberto Ferroni[‡], Ilario Mazzieri[‡], Alfio Quarteroni[‡]

October 4, 2016

[‡] MOX, Dipartimento di Matematica, Politecnico di Milano, Piazza Leonardo da Vinci 32, 20133 Milano, Italy

`paola.antonietti@polimi.it`, `alberto.ferroni@polimi.it`,
`ilario.mazzieri@polimi.it`

[‡] CMCS, Ecole Polytechnique Federale de Lausanne (EPFL), Station 8, 1015 Lausanne, Switzerland

`alfio.quarteroni@epfl.ch`

Abstract

In this paper we extend the results contained in [1] and consider the problem of approximating the elastodynamics equation by means of *hp*-version discontinuous Galerkin methods. For the resulting semi-discretized schemes we derive stability bounds as well as *hp* error estimates in a suitable energy norm. Our theoretical estimates are verified through three dimensions numerical experiments.

Introduction

The present paper deals with the numerical modeling through the (linear) elastodynamics equation of seismic wave propagation phenomena in complex, three-dimensional media. Currently, the numerical methods mostly employed to tackle seismic wave propagation include finite differences, pseudo-spectral, spectral element, and high-order/spectral element discontinuous (DG) Galerkin techniques. In particular Spectral Element methods, firstly introduced for fluid dynamics problems in the seminal paper [17], have become one of the most effective and powerful approaches for solving three-dimensional seismic wave propagation problems in strongly heterogeneous media thanks to their geometrical flexibility and high order accuracy, which made them well suited

*P.A. and I.M. have been partially supported by the research grant no. 2015-0182 funded by Fondazione Cariplo and Regione Lombardia. Part of this work has been completed while P.A. was visiting the Institut Henri Poincaré (IHP), Paris. She thanks the Institute for the kind hospitality.

to correctly approximate the wave field. We refer to [7, 12, 14, 15, 24] for the first development of Spectral Element methods for the elastodynamics equation, and, for example, to [11, 13, 25, 28] for its application in computational seismology. In recent years, *displacement-based* high-order/spectral element discontinuous Galerkin methods have also been developed for linear and nonlinear (visco) elastic wave propagation problems, mainly because the discretization parameters, i.e. the mesh-size and/or the polynomial approximation degree, can be naturally tailored to the region of interests; another interesting feature is their being embarrassingly parallel and therefore naturally oriented towards high performance parallel computing, see e.g. Their are thus very well suited to deal with *i)* the intrinsic multi-scale nature of seismic wave propagation problems, involving a relative broad range of wavelengths; *ii)* the complexity of the geometrical constraints. The aim of this paper is to extend to the *hp*-version the theoretical analysis developed in [1] as well as to prove approximation bounds in the L^2 norm. For the sake of brevity, here we focus only on *displacement* DG formulation, but the present analysis can be extended also to *displacement-stress* formulations. We show that, also in the *hp*-version setting, stability and approximation properties hold without the need of introducing an extra term that penalizes the time derivative of the displacement besides the displacement itself, as considered in previous works [20–22]. Our semidiscrete analysis represents an intermediate but essential step towards the analysis of stability of the fully discrete scheme resulting after time integration.

The remaining part of manuscript is organized as follows. In Section 1 we introduce the model problem and its *hp*-version discontinuous Galerkin approximation. The stability analysis is presented in Section 2, whereas in Section 3 we present the *hp*-version *a priori* error estimates in both the energy and L^2 norms. Three-dimensional numerical experiments verifying the theory are presented in Section 4.

1 Problem statement and its *hp*-version discontinuous Galerkin approximation

Let $\Omega \subset \mathbf{R}^d$, $d = 2, 3$, be an open, bounded convex region with Lipschitz boundary $\partial\Omega$. Throughout the paper, $[H^m(\Omega)]^d$ and $[H^m(\Omega)]_{\text{sym}}^{d \times d}$ denote the standard Sobolev spaces of vector-valued and symmetric tensor-valued functions defined over Ω , respectively, and $(\cdot, \cdot)_\Omega$ denote the standard inner product in any of the spaces $[L^2(\Omega)]^d$ or $[L^2(\Omega)]_{\text{sym}}^{d \times d}$. For given $T > 0$ and $\mathbf{f} = \mathbf{f}(x, t) \in L^2((0, T]; [L^2(\Omega)]^d)$, we consider the problem of approximating the variational formulation of the linear elastodynamics equation with homogenous Dirichlet boundary conditions: for all $t \in (0, T]$ find $\mathbf{u} = \mathbf{u}(t) \in \mathbf{V} \equiv [H_0^1(\Omega)]^d$ such that:

$$(\rho \mathbf{u}_{tt}, \mathbf{v})_\Omega + (\mathcal{D}\boldsymbol{\varepsilon}(\mathbf{u}), \boldsymbol{\varepsilon}(\mathbf{v}))_\Omega = (\mathbf{f}, \mathbf{v})_\Omega \quad \forall \mathbf{v} \in \mathbf{V}, \quad (1)$$

subjected to the (regular enough) initial conditions \mathbf{u}_0 and \mathbf{u}_1 . Here, $\mathbf{u} : \Omega \times [0, T] \rightarrow \mathbb{R}^d$ is the displacement vector field and $\varepsilon(\mathbf{u}) : \Omega \rightarrow \mathbb{R}_{\text{sym}}^{d \times d}$ is the symmetric gradient. Moreover, ρ is the mass density, which is supposed to be a strictly positive and uniformly bounded function, and $\mathcal{D} = \mathcal{D}(x) : \mathbb{R}_{\text{sym}}^{d \times d} \rightarrow \mathbb{R}_{\text{sym}}^{d \times d}$ is the inverse of the *compliance* tensor defined as $\mathcal{D}\boldsymbol{\tau} = 2\mu\boldsymbol{\tau} + \lambda \text{tr}(\boldsymbol{\tau})\mathbb{I} \quad \forall \boldsymbol{\tau} \in \mathbb{R}_{\text{sym}}^{d \times d}$. $\mathbb{I} \in \mathbb{R}^{d \times d}$ and $\text{tr}(\cdot)$ are the identity and trace operators, respectively, and $\lambda, \mu \in L^\infty(\Omega)$, $\lambda, \mu > 0$, being the Lamé parameters.

Henceforth, C denotes a generic positive constant independent of the discretization parameters, but that can depend on the physical quantities ρ, \mathcal{D} as well as on the final observation time T . Moreover, $x \lesssim y$ and $x \gtrsim y$ will signify $x \leq Cy$ and $x \geq Cy$, respectively, with C as before.

1.1 Mesh, trace operators, and discrete spaces

We consider a sequence $\{\mathcal{T}_h\}_h$ of shape-regular (not-necessarily matching) partitions of Ω into disjoint open elements K such that $\bar{\Omega} = \cup_{K \in \mathcal{T}_h} \bar{K}$, where each $K \in \mathcal{T}_h$ is the affine image of a fixed master element \hat{K} , *i.e.*, $K = F_K(\hat{K})$, \hat{K} being either the open unit d -simplex or the open unit hypercube in \mathbb{R}^d , $d = 2, 3$. An interior face (for $d = 2$, “face” means “edge”) of \mathcal{T}_h is defined as the (non-empty) interior of $\partial\bar{K}^+ \cap \partial\bar{K}^-$, where K^\pm are two adjacent elements of \mathcal{T}_h . Similarly, a boundary face of \mathcal{T}_h is defined as the (non-empty) interior of $\partial\bar{K} \cap \bar{\Omega}$, where K is a boundary element of \mathcal{T}_h . We collect the interior and boundary faces in the sets \mathcal{F}_h^I and \mathcal{F}_h^B , respectively, and define $\mathcal{F}_h = \mathcal{F}_h^I \cup \mathcal{F}_h^B$. We also assume the following mesh-regularity: *i)* for any $K \in \mathcal{T}_h$ and for all $F \in \mathcal{F}_h$, $F \subset \partial K$, $h_K \lesssim h_F$; *ii)* for any pair of elements $K^\pm \in \mathcal{T}_h$ sharing a $(d-1)$ -dimensional face $h_{K^-} \lesssim h_{K^+} \lesssim h_{K^-}$: cf. [8, 18] for example.

Next, we introduce suitable trace operators, cf. [3, 4]. Let F be an interior face shared by two elements K^\pm of \mathcal{T}_h , and let \mathbf{n}^\pm denote the normal unit vectors on F pointing outward K^\pm , respectively. For (regular enough) vector-valued and symmetric tensor-valued functions \mathbf{v} and $\boldsymbol{\tau}$, respectively, we define the *weighted average* and *jump* operators as

$$\begin{aligned} \{\mathbf{v}\}_\delta &= \delta \mathbf{v}^+ + (1 - \delta) \mathbf{v}^-, & \{\boldsymbol{\tau}\}_\delta &= \delta \boldsymbol{\tau}^+ + (1 - \delta) \boldsymbol{\tau}^-, & \delta &\in [0, 1], \\ \llbracket \mathbf{v} \rrbracket &= \mathbf{v}^+ \odot \mathbf{n}^+ + \mathbf{v}^- \odot \mathbf{n}^-, & \llbracket \boldsymbol{\tau} \rrbracket &= \boldsymbol{\tau}^+ \mathbf{n}^+ + \boldsymbol{\tau}^- \mathbf{n}^-, \end{aligned} \tag{2}$$

where \mathbf{v}^\pm and $\boldsymbol{\tau}^\pm$ denote the traces of \mathbf{v} and $\boldsymbol{\tau}$ on F taken within the interior of K^\pm , respectively, and where $\mathbf{v} \odot \mathbf{n} = (\mathbf{v}\mathbf{n}^T + \mathbf{n}\mathbf{v}^T)/2$. Notice that $\llbracket \mathbf{v} \rrbracket$ is a symmetric tensor-valued function. On a boundary face $F \in \mathcal{F}_h^B$, we set analogously

$$\{\mathbf{v}\}_\delta = \mathbf{v}, \quad \{\boldsymbol{\tau}\}_\delta = \boldsymbol{\tau}, \quad \llbracket \mathbf{v} \rrbracket = \mathbf{v} \odot \mathbf{n}, \quad \llbracket \boldsymbol{\tau} \rrbracket = \boldsymbol{\tau} \mathbf{n}. \tag{3}$$

When $\delta = 1/2$, we drop the subindex and simply write $\{\cdot\}$.

Finally, to any element $K \in \mathcal{T}_h$ we assign a polynomial approximation degree $p_K \geq 1$, and define the hp -discontinuous finite element space

$$\mathbf{V}_{hp} = \{\mathbf{u} \in [L^2(\Omega)]^d : \mathbf{u} \circ F_K \in [\mathbb{M}^{p_K}(\widehat{K})]^d \quad \forall K \in \mathcal{T}_h\},$$

where $\mathbb{M}^{p_K}(\widehat{K})$ is either the space $\mathbb{P}^{p_K}(\widehat{K})$ of polynomials of degree at most p_K on \widehat{K} , if \widehat{K} is the reference d -simplex, or the space $\mathbb{Q}^{p_K}(\widehat{K})$ of tensor-product polynomials on \widehat{K} of degree p_K in each coordinate direction, if \widehat{K} is the unit reference hypercube in \mathbb{R}^d . In the following we also assume that the following *local bounded* variation holds: $p_{K^-} \lesssim p_{K^+} \lesssim p_{K^-}$ for any pair of elements $K^\pm \in \mathcal{T}_h$ sharing a $(d-1)$ -dimensional face, cf. [18] for example.

Given a face $F \in \mathcal{F}_h$ of an element $K \in \mathcal{T}_h$, i.e., $F \subset \partial K$ the following inverse inequality holds:

$$\|v\|_{L^2(F)}^2 \lesssim \frac{p_K^2}{h_K} \|v\|_{L^2(K)}^2 \quad \forall v \in \mathbb{M}^{p_K}(K),$$

cf. [23]. Finally, we recall the following interpolation estimates, cf. [23], for example.

Lemma 1.1. *For any real number $s_K \geq 0$ and for any function $\mathbf{v} \in [H^{s_K}(K)]^d$, $K \in \mathcal{T}_h$, there exists $\Pi_h \mathbf{v} \in \mathbf{V}_{hp}$ such that*

$$\sum_{K \in \mathcal{T}_h} \|\mathbf{v} - \Pi_h \mathbf{v}\|_{H^r(K)} \lesssim \sum_{K \in \mathcal{T}_h} \frac{h_K^{\min(s_K, p_K + 1) - r}}{p_K^{s_K - r}} \|\mathbf{v}\|_{H^{s_K}(K)}$$

for all r , $0 \leq r \leq s_K$, and

$$\sum_{K \in \mathcal{T}_h} \|D^\xi(\mathbf{v} - \Pi_h \mathbf{v})\|_{L^2(\partial K)} \lesssim \sum_{K \in \mathcal{T}_h} \frac{h_K^{\min(s_K, p_K + 1) - |\xi| - 1/2}}{p_K^{s_K - |\xi| - 1/2}} \|\mathbf{v}\|_{H^{s_K}(K)}$$

for all ξ , $0 \leq |\xi| \leq k$, where $\xi \in \mathbb{N}_0^d$ is a multi-index of length $|\xi|$. Here, the second inequality holds provided $s_K > 1/2$ and k is the largest non-negative integer strictly less than $s - 1/2$.

1.2 Semi-discrete formulation

We are now ready to state the semi-discrete weak formulation: For any time $t \in (0, T]$, find $\mathbf{u}^h = \mathbf{u}^h(t) \in \mathbf{V}_{hp}$ such that

$$(\rho \mathbf{u}_{tt}^h, \mathbf{v})_{\mathcal{T}_h} + \mathcal{A}(\mathbf{u}^h, \mathbf{v}) = (\mathbf{f}, \mathbf{v})_{\mathcal{T}_h} \quad \forall \mathbf{v} \in \mathbf{V}_{hp}, \quad (4)$$

subjected to the initial conditions \mathbf{u}_0^h and \mathbf{u}_1^h , being $\mathbf{u}_0^h, \mathbf{u}_1^h \in \mathbf{V}_{hp}$ suitable approximations in \mathbf{V}_{hp} of the initial data $\mathbf{u}_0, \mathbf{u}_1$, respectively. The bilinear form $\mathcal{A}(\cdot, \cdot) : \mathbf{V}_{hp} \times \mathbf{V}_{hp} \rightarrow \mathbb{R}$ in (13) is given by

$$\begin{aligned} \mathcal{A}(\mathbf{w}, \mathbf{v}) &= (\boldsymbol{\varepsilon}(\mathbf{w}), \mathcal{D}\boldsymbol{\varepsilon}(\mathbf{v}))_{\mathcal{T}_h} - \langle \{\mathcal{D}\boldsymbol{\varepsilon}(\mathbf{w})\}_\delta, \llbracket \mathbf{v} \rrbracket \rangle_{\mathcal{F}_h} \\ &\quad - \langle \llbracket \mathbf{w} \rrbracket, \{\mathcal{D}\boldsymbol{\varepsilon}(\mathbf{v})\}_\delta \rangle_{\mathcal{F}_h} + \langle \sigma \llbracket \mathbf{w} \rrbracket, \llbracket \mathbf{v} \rrbracket \rangle_{\mathcal{F}_h}, \end{aligned} \quad (5)$$

where we have used the shorthand notation $(\mathbf{w}, \mathbf{v})_{\mathcal{T}_h} = \sum_{K \in \mathcal{T}_h} (\mathbf{w}, \mathbf{v})_K$ and $(\mathbf{w}, \mathbf{v})_{\mathcal{F}_h} = \sum_{F \in \mathcal{F}_h} (\mathbf{w}, \mathbf{v})_F$. The above method corresponds to the family of Interior Penalty (IP) methods: for $\delta = 1/2$, we get the Symmetric Interior Penalty (SIP) method [2, 29], whereas for $\delta \neq 1/2$ we obtain the *weighted* SIP method of Stenberg, [27]. In (5) the stabilization function $\sigma \in L^\infty(\mathcal{F}_h)$ is defined facewise as

$$\sigma = \sigma(x) = \begin{cases} \alpha\{\mathcal{D}\} \frac{\max(p_{K^+}^2, p_{K^-}^2)}{\min(h_{K^+}, h_{K^-})} & \text{if } x \in \overline{\partial K^+} \cap \overline{\partial K^-}, \\ \alpha\{\mathcal{D}\} \frac{p_K^2}{h_K} & \text{if } x \in \overline{\partial K} \cap \partial\Omega, \end{cases} \quad (6)$$

By defining $[H^s(\mathcal{T}_h)]^d$ as the space of elementwise $[H^s(K)]^d$ functions, $s \geq 0$, and endowing the \mathbf{V}_{hp} and $\mathbf{V}_{hp} + [H^2(\mathcal{T}_h)]^d$ spaces with the (mesh-dependent) norms

$$\begin{aligned} \|\mathbf{v}\|_{\text{DG}}^2 &= \|\mathcal{D}^{1/2} \boldsymbol{\varepsilon}(\mathbf{v})\|_{L^2(\mathcal{T}_h)}^2 + \|\sigma^{1/2} \llbracket \mathbf{v} \rrbracket\|_{L^2(\mathcal{F}_h)}^2 \quad \forall \mathbf{v} \in \mathbf{V}_{hp}, \\ \|\mathbf{v}\|_{\text{DG}}^2 &= \|\mathbf{v}\|_{\text{DG}}^2 + \|\sigma^{-1/2} \{\boldsymbol{\varepsilon}(\mathbf{v})\}\|_{L^2(\mathcal{F}_h)}^2 \quad \forall \mathbf{v} \in \mathbf{V}_{hp} + [H^2(\mathcal{T}_h)]^d, \end{aligned} \quad (7)$$

respectively, with $\|\mathbf{w}\|_{L^2(\mathcal{T}_h)} = \sqrt{(\mathbf{w}, \mathbf{w})_{\mathcal{T}_h}}$ and $\|\mathbf{w}\|_{L^2(\mathcal{F}_h)} = \sqrt{(\mathbf{w}, \mathbf{w})_{\mathcal{F}_h}}$, with standard arguments it is easy to prove the following result.

Lemma 1.2. *The bilinear form $\mathcal{A}(\cdot, \cdot) : \mathbf{V}_{hp} \times \mathbf{V}_{hp} \rightarrow \mathbb{R}$ defined as in (5) satisfies*

$$|\mathcal{A}(\mathbf{w}, \mathbf{v})| \lesssim \|\mathbf{v}\|_{\text{DG}} \|\mathbf{w}\|_{\text{DG}}, \quad \mathcal{A}(\mathbf{v}, \mathbf{v}) \gtrsim \|\mathbf{v}\|_{\text{DG}}^2 \quad \forall \mathbf{w}, \mathbf{v} \in \mathbf{V}_{hp},$$

where the second estimates holds provided that the penalty parameter α is chosen large enough, cf. (6). Moreover,

$$|\mathcal{A}(\mathbf{w}, \mathbf{v})| \lesssim \|\mathbf{v}\|_{\text{DG}} \|\mathbf{w}\|_{\text{DG}}, \quad \forall \mathbf{w}, \mathbf{v} \in \mathbf{V}_{hp} + [H^2(\mathcal{T}_h)]^d.$$

2 Stability of the semi-discrete formulation

We now prove stability in the following natural energy norm induced by the DG methods described in the previous section:

$$\|\mathbf{v}\|_{\mathbb{E}}^2 = \|\rho^{1/2} \mathbf{v}_t\|_{0, \mathcal{T}_h}^2 + \|\mathbf{v}\|_{\text{DG}}^2 \quad \forall \mathbf{v} = \mathbf{v}(t) \in C^2([0, T]; \mathbf{V}_{hp}) \quad \forall t \in [0, T]. \quad (8)$$

First, we recall the following classical result, cf. [19, pag. 28].

Lemma 2.1. *Let $\xi \in L^2(0, T)$ a positive function and $\eta \in C^0(0, T)$ a non-negative function such that*

$$\eta^2(t) \leq C + \int_0^t \xi(\tau) \eta(\tau) d\tau \quad \forall t \in (0, T)$$

with C a non-negative constant. Then,

$$\eta(t) \leq \sqrt{C} + \frac{1}{2} \int_0^t \xi(\tau) d\tau \quad \forall t \in (0, T)$$

For the forthcoming analysis we will assume that the (possible) discontinuities of the piecewise constant stiffness tensor \mathcal{D} are aligned with the mesh partition \mathcal{T}_h .

Proposition 2.2. *Let $\mathbf{u}^h \in C^2((0, T]; \mathbf{V}_{hp})$ be the approximate solution obtained with the SIP(δ) method (13), for a sufficiently large penalty parameter α , cf. (6). Then,*

$$\|\mathbf{u}^h(t)\|_{\mathbb{E}} \lesssim \|\mathbf{u}^h(0)\|_{\mathbb{E}} + \int_0^t \|\mathbf{f}(\tau)\|_{L^2(\Omega)} d\tau \quad 0 < t \leq T.$$

Proof. We take $\mathbf{v} = \mathbf{u}_t^h \in \mathbf{V}_{hp}$ in (13) to obtain

$$\frac{1}{2} \frac{d}{dt} (\|\mathbf{u}^h\|_{\mathbb{E}}^2 - 2\langle \{\mathcal{D}\boldsymbol{\varepsilon}(\mathbf{u}^h)\}_{\delta}, [\![\mathbf{u}^h]\!] \rangle_{\mathcal{F}_h}) = (\mathbf{f}, \mathbf{u}_t^h)_{\mathcal{T}_h}. \quad (9)$$

Integrating in time between 0 and t leads to

$$\begin{aligned} \|\mathbf{u}^h\|_{\mathbb{E}}^2 - 2\langle \{\mathcal{D}\boldsymbol{\varepsilon}(\mathbf{u}^h)\}_{\delta}, [\![\mathbf{u}^h]\!] \rangle_{\mathcal{F}_h} &= \|\mathbf{u}_0^h\|_{\mathbb{E}}^2 - 2\langle \{\mathcal{D}\boldsymbol{\varepsilon}(\mathbf{u}^h(0))\}_{\delta}, [\![\mathbf{u}^h(0)]\!] \rangle_{\mathcal{F}_h} \\ &\quad + 2 \int_0^t (\mathbf{f}, \mathbf{u}_\tau^h)_{\mathcal{T}_h} d\tau. \end{aligned} \quad (10)$$

We first observe that, for any $F \in \mathcal{F}_h$, and any $\mathbf{w}, \mathbf{v} \in \mathbf{V}_{hp}$, the Cauchy-Schwarz inequality gives

$$\begin{aligned} \sum_{F \in \mathcal{F}_h} |\langle \{\mathcal{D}\boldsymbol{\varepsilon}(\mathbf{w})\}_{\delta}, [\![\mathbf{v}]\!] \rangle_F| &\leq \|\sigma^{-1/2} \{\mathcal{D}\boldsymbol{\varepsilon}(\mathbf{w})\}\|_{0, \mathcal{F}_h} \|\sigma^{1/2} [\![\mathbf{v}]\!] \|_{0, \mathcal{F}_h} \\ &\lesssim \frac{1}{\sqrt{\alpha}} \|\mathcal{D}^{1/2} \boldsymbol{\varepsilon}(\mathbf{w})\|_{0, \mathcal{T}_h} \|\sigma^{1/2} [\![\mathbf{v}]\!] \|_{0, \mathcal{F}_h} \\ &\leq \frac{1}{\sqrt{\alpha}} \|\mathbf{w}\|_{\text{DG}} \|\mathbf{v}\|_{\text{DG}} \leq \frac{1}{\sqrt{\alpha}} \|\mathbf{w}\|_{\mathbb{E}} \|\mathbf{v}\|_{\mathbb{E}}, \end{aligned}$$

where in the second step we have employed the definition (6) of the penalty function σ , the local bounded variation property of the discretization parameters, together with the trace-inverse inequality (1.1). From the Young inequality, we obtain

$$\|\mathbf{u}^h\|_{\mathbb{E}}^2 - 2\langle \{\mathcal{D}\boldsymbol{\varepsilon}(\mathbf{u}^h)\}_{\delta}, [\![\mathbf{u}^h]\!] \rangle_{\mathcal{F}_h} \gtrsim \|\mathbf{u}^h\|_{\mathbb{E}}^2,$$

provided that the penalty parameter α is chosen sufficiently large. This leads to

$$\|\mathbf{u}^h\|_{\mathbb{E}}^2 \lesssim \|\mathbf{u}^h(0)\|_{\mathbb{E}}^2 + \int_0^t (\mathbf{f}, \mathbf{u}_\tau^h)_{\mathcal{T}_h} d\tau.$$

Next, we observe that, from the Cauchy-Schwarz inequality we have

$$\int_0^t (\mathbf{f}, \mathbf{u}_\tau^h)_{\mathcal{T}_h} d\tau \leq \int_0^t \|\mathbf{f}\|_{\mathcal{T}_h, 0} \|\rho^{1/2} \mathbf{u}_\tau^h\|_{\mathcal{T}_h, 0} d\tau \leq \int_0^t \|\mathbf{f}\|_{\mathcal{T}_h, 0} \|\mathbf{u}^h\|_{\mathbb{E}} d\tau,$$

which leads to

$$\|\mathbf{u}^h(t)\|_{\mathbb{E}}^2 \lesssim \|\mathbf{u}^h(0)\|_{\mathbb{E}}^2 + \int_0^t \|\mathbf{f}\|_{\mathcal{T}_h, 0} \|\mathbf{u}^h\|_{\mathbb{E}} d\tau.$$

The thesis follows by Lemma 2.1. \square

3 Error analysis

Before stating the main result of this section, we recall some preliminary results that will be needed for the forthcoming analysis.

Lemma 3.1. *For any $\mathbf{v} \in [H^{s_K}(K)]^d$, $s_K \geq 0$, $K \in \mathcal{T}_h$, there exists $\Pi_{hp}\mathbf{v} \in \mathbf{V}_{hp}$ s.t.*

$$\|\mathbf{v} - \Pi_{hp}\mathbf{v}\|_{\text{DG}}^2 \lesssim \sum_{K \in \mathcal{T}_h} \frac{h_K^{2\min(s_K, p_K+1)-2}}{p_K^{2s_K-3}} \|\mathbf{v}\|_{H^{s_K}(K)}^2. \quad (11)$$

Moreover, if $\mathbf{v}, \mathbf{v}_t \in [H^{s_K}(K)]^d$, for any $K \in \mathcal{T}_h$, then

$$\|\mathbf{v} - \Pi_{hp}\mathbf{v}\|_{\text{E}}^2 \lesssim \sum_{K \in \mathcal{T}_h} \frac{h_K^{2\min(s_K, p_K+1)-2}}{p_K^{2s_K-3}} \left(\|\mathbf{v}_t\|_{H^{s_K}(K)}^2 + \|\mathbf{v}\|_{H^{s_K}(K)}^2 \right). \quad (12)$$

Proof. We only show (12), as (11) is a particular case. Recalling the definition of the energy norm $\|\cdot\|_{\text{E}}$ and employing the estimates of Lemma 1.1 we obtain

$$\begin{aligned} \|\rho^{1/2}(\mathbf{v}_t - \Pi_{hp}\mathbf{v}_t)\|_{0, \mathcal{T}_h}^2 &\lesssim \sum_{K \in \mathcal{T}_h} \frac{h_K^{2\min(s_K, p_K+1)}}{p_K^{2s_K}} \|\mathbf{v}_t\|_{H^{s_K}(K)}^2, \\ \|\mathcal{D}^{1/2}\boldsymbol{\varepsilon}(\mathbf{v} - \Pi_{hp}\mathbf{v})\|_{L^2(\mathcal{T}_h)}^2 &\lesssim \sum_{K \in \mathcal{T}_h} \frac{h_K^{2\min(s_K, p_K+1)-2}}{p_K^{2s_K-2}} \|\mathbf{v}\|_{H^{s_K}(K)}^2, \\ \|\sigma^{1/2}[\mathbf{v} - \Pi_{hp}\mathbf{v}]\|_{L^2(\mathcal{F}_h)}^2 &\lesssim \sum_{K \in \mathcal{T}_h} \frac{h_K^{2\min(s_K, p_K+1)-2}}{p_K^{2s_K-3}} \|\mathbf{v}\|_{H^{s_K}(K)}^2, \end{aligned}$$

that is

$$\begin{aligned} \|\mathbf{v} - \Pi_{hp}\mathbf{v}\|_{\text{E}}^2 &\lesssim \sum_{K \in \mathcal{T}_h} \frac{h_K^{2\min(s_K, p_K+1)-2}}{p_K^{2s_K-3}} \left(\frac{h_K^2}{p_K^3} \|\mathbf{v}_t\|_{H^{s_K}(K)}^2 \right. \\ &\quad \left. + \frac{1}{p_K} \|\mathbf{v}\|_{H^{s_K}(K)}^2 + \|\mathbf{v}\|_{H^{s_K}(K)}^2 \right) \\ &\lesssim \sum_{K \in \mathcal{T}_h} \frac{h_K^{2\min(s_K, p_K+1)-2}}{p_K^{2s_K-3}} (\|\mathbf{v}_t\|_{H^{s_K}(K)}^2 + \|\mathbf{v}\|_{H^{s_K}(K)}^2), \end{aligned}$$

where the last step follows by observing that $\frac{h_K^2}{p_K^3} < 1$ and $\frac{1}{p_K} < 1$ for any $K \in \mathcal{T}_h$. \square

3.1 Error estimates in the energy norm

In this section we present *a priori* error estimates in the natural energy norm. Assuming that the exact solution \mathbf{u} is regular enough, i.e., $\mathbf{u}|_K \in [H^{s_K}(K)]^d$ for any $K \in \mathcal{T}_h$, with $s_K \geq 2$, with standard arguments it

is also possible to show that formulation (13) is *strongly consistent*, i.e.,

$$(\rho \mathbf{u}_{tt}, \mathbf{v})_{\mathcal{T}_h} + \mathcal{A}(\mathbf{u}, \mathbf{v}) = (\mathbf{f}, \mathbf{v})_{\mathcal{T}_h} \quad \forall \mathbf{v} \in \mathbf{V}_{hp}. \quad (13)$$

From the above identity, we can obtain the following relation for the error $\mathbf{e} = \mathbf{u} - \mathbf{u}^h$

$$(\rho \mathbf{e}_{tt}, \mathbf{v})_{\mathcal{T}_h} + \mathcal{A}(\mathbf{e}, \mathbf{v}) = \mathbf{0} \quad \forall \mathbf{v} \in \mathbf{V}_{hp}, \quad (14)$$

which serves as the basis for the forthcoming error estimates.

Theorem 3.2. (*A-priori error estimate in the energy norm.*) *Let \mathbf{u} be the exact solution of problem (1) and let \mathbf{u}^h be its approximation based on employing the semidiscrete DG formulation given in (13), with a penalty parameter α chosen large enough, cf. (6). If, for any time $t \in [0, T]$, the exact solution $\mathbf{u}(t)$ and its two first temporal derivatives belong $[H^{s_K}(K)]^d$, $K \in \mathcal{T}_h$, $s_K \geq 2$, then*

$$\begin{aligned} \sup_{t \in (0, T]} \|\mathbf{e}(t)\|_{\mathbb{E}}^2 &\lesssim \sup_{t \in (0, T]} \left\{ \sum_{K \in \mathcal{T}_h} \frac{h_K^{2 \min(s_K, p_K + 1) - 2}}{p_K^{2s_K - 3}} \left(\|\mathbf{u}_t(t)\|_{H^{s_K}(K)}^2 \right. \right. \\ &\quad \left. \left. + \|\mathbf{u}(t)\|_{H^{s_K}(K)}^2 \right) \right\} \\ &+ \int_0^T \sum_{K \in \mathcal{T}_h} \left\{ \frac{h_K^{2 \min(s_K, p_K + 1) - 2}}{p_K^{2s_K - 3}} \left(\|\mathbf{u}_{tt}(\tau)\|_{H^{s_K}(K)}^2 \right. \right. \\ &\quad \left. \left. + \|\mathbf{u}_t(\tau)\|_{H^{s_K}(K)}^2 \right) \right\} d\tau. \end{aligned}$$

Before reporting the proof of Theorem 3.2 we recall the integration by parts formula

$$\int_0^t (\mathbf{w}, \mathbf{v}_\tau)_* d\tau = (\mathbf{w}(t), \mathbf{v}(t))_* - (\mathbf{w}(0), \mathbf{v}(0))_* - \int_0^t (\mathbf{w}_\tau, \mathbf{v})_* d\tau, \quad (15)$$

that holds for \mathbf{w}, \mathbf{v} regular enough and for any scalar product $(\cdot, \cdot)_*$

Proof. Let $\Pi_{hp} \mathbf{u} \in \mathbf{V}_{hp}$ be the interpolant defined as in Lemma 3.1. By decomposing the error as $\mathbf{e} = \mathbf{e}^\pi - \mathbf{e}^h$, with $\mathbf{e}^\pi = \mathbf{u} - \Pi_{hp} \mathbf{u}$ and $\mathbf{e}^h = \mathbf{u}^h - \Pi_{hp} \mathbf{u}$, (14) becomes:

$$(\rho \mathbf{e}_{tt}^h, \mathbf{v})_{\mathcal{T}_h} + \mathcal{A}(\mathbf{e}^h, \mathbf{v}) = (\rho \mathbf{e}_{tt}^\pi, \mathbf{v})_{\mathcal{T}_h} + \mathcal{A}(\mathbf{e}^\pi, \mathbf{v}) \quad \forall \mathbf{v} \in \mathbf{V}_{hp}.$$

By taking $\mathbf{v} = \mathbf{e}^h$ in the above identity, we have

$$\frac{1}{2} \frac{d}{dt} (\|\mathbf{e}^h\|_{\mathbb{E}}^2 - 2\langle \llbracket \mathbf{e}^h \rrbracket, \{\mathcal{D}\varepsilon(\mathbf{e}^h)\}_\delta \rangle_{\mathcal{F}_h}) = (\rho \mathbf{e}_{tt}^\pi, \mathbf{e}_t^h)_{\mathcal{T}_h} + \mathcal{A}(\mathbf{e}^\pi, \mathbf{e}_t^h). \quad (16)$$

Reasoning as in the proof of Theorem 2.2, we have

$$\|\mathbf{e}^h\|_{\mathbb{E}}^2 - 2\langle \llbracket \mathbf{e}^h \rrbracket, \{\mathcal{D}\varepsilon(\mathbf{e}^h)\}_\delta \rangle_{\mathcal{F}_h} \gtrsim \|\mathbf{e}^h\|_{\mathbb{E}}^2,$$

provided that the penalty parameter α is chosen large enough; cf. (6). Integrating (16) in time between 0 and t and using that $\mathbf{e}^h(0) = \mathbf{u}^h(0) - \mathbf{u}^\pi(0) = \mathbf{0}$, we get

$$\begin{aligned} \|\mathbf{e}^h\|_{\mathbb{E}}^2 &\lesssim \int_0^t (\rho \mathbf{e}_{tt}^\pi, \mathbf{e}_t^h)_{\mathcal{T}_h} d\tau + \int_0^t \mathcal{A}(\mathbf{e}^\pi, \mathbf{e}_t^h) d\tau \\ &\lesssim \int_0^t \|\mathbf{e}_t^\pi\|_{\mathbb{E}} \|\mathbf{e}^h\|_{\mathbb{E}} d\tau + \mathcal{A}(\mathbf{e}^\pi, \mathbf{e}^h) - \int_0^t \mathcal{A}(\mathbf{e}_t^\pi, \mathbf{e}^h) d\tau \\ &\lesssim \int_0^t \|\mathbf{e}_t^\pi\|_{\mathbb{E}} \|\mathbf{e}^h\|_{\mathbb{E}} d\tau + \|\mathbf{e}^\pi\|_{\text{DG}} \|\mathbf{e}^h\|_{\text{DG}} + \int_0^t \|\mathbf{e}_t^\pi\|_{\text{DG}} \|\mathbf{e}^h\|_{\text{DG}} d\tau, \end{aligned} \quad (17)$$

where the second step follows based on employing the Cauchy-Schwarz inequality together with integration by parts formula (15) with $\mathbf{w} = \mathbf{e}^\pi$, $\mathbf{v} = \mathbf{e}^h$ and $(\cdot, \cdot)_* = \mathcal{A}(\cdot, \cdot)$, whereas the third one follows from Lemma (7). From the Young inequality

$$\|\mathbf{e}^\pi\|_{\text{DG}} \|\mathbf{e}^h\|_{\text{DG}} \leq \frac{1}{\epsilon} \|\mathbf{e}^\pi\|_{\text{DG}}^2 + \epsilon \|\mathbf{e}^h\|_{\text{DG}}^2 \leq \frac{1}{\epsilon} \|\mathbf{e}^\pi\|_{\text{DG}}^2 + \epsilon \|\mathbf{e}^h\|_{\mathbb{E}}^2,$$

we can suitably choose ϵ and rewrite (22) as

$$\|\mathbf{e}^h\|_{\mathbb{E}}^2 \lesssim \|\mathbf{e}^\pi\|_{\text{DG}}^2 + \int_0^t (\|\mathbf{e}_t^\pi\|_{\text{DG}} + \|\mathbf{e}_t^\pi\|_{\mathbb{E}}) \|\mathbf{e}^h\|_{\text{DG}} d\tau. \quad (18)$$

Applying Gronwall's Lemma 2.1 we get

$$\|\mathbf{e}^h(t)\|_{\mathbb{E}} \lesssim \sup_{t \in [0, T]} \|\mathbf{e}^\pi(t)\|_{\text{DG}}^2 + \int_0^t \|\mathbf{e}_t^\pi(\tau)\|_{\mathbb{E}} d\tau \quad \forall t \in (0, T].$$

Finally, from the Cauchy-Schwarz inequality and the above bound, and taking the supremum over $t \in (0, T]$

$$\sup_{t \in (0, T]} \|\mathbf{e}(t)\|_{\mathbb{E}}^2 \lesssim \sup_{t \in (0, T]} \{ \|\mathbf{e}^\pi(t)\|_{\mathbb{E}}^2 + \|\mathbf{e}^\pi(t)\|_{\text{DG}}^2 \} + \int_0^T \|\mathbf{e}_t^\pi(\tau)\|_{\mathbb{E}}^2 d\tau.$$

The proof is completed by applying Lemma 3.1. \square

Remark 3.3. *If the mesh size is quasi uniform, i.e. $h = \max_{K \in \mathcal{T}_K} h_K \approx h_K$ for any $K \in \mathcal{T}_h$, the polynomial approximation degree is uniform, i.e. $p_K = p$ for any $K \in \mathcal{T}_h$, and the exact solution satisfies $\mathbf{u}|_K, \mathbf{u}_t|_K, \mathbf{u}_{tt}|_K \in [H^s(K)]^d$ for any $K \in \mathcal{T}_h$ and for any $t \in [0, T]$, with $s \geq p + 1$, the error estimate of Theorem 3.2 becomes*

$$\begin{aligned} \sup_{t \in (0, T]} \|\mathbf{e}(t)\|_{\mathbb{E}}^2 &\lesssim \frac{h^{2p}}{p^{2s-3}} \sup_{t \in (0, T]} \left\{ \|\mathbf{u}_t(t)\|_{H^s(\Omega)}^2 + \|\mathbf{u}(t)\|_{H^s(\Omega)}^2 \right\} \\ &\quad + \frac{h^{2p}}{p^{2s-3}} \int_0^T \left\{ \|\mathbf{u}_{tt}(\tau)\|_{H^s(\Omega)}^2 + \|\mathbf{u}_t(\tau)\|_{H^s(\Omega)}^2 \right\} d\tau. \end{aligned}$$

The above bounds are optimal in h and suboptimal in p by a factor $p^{1/2}$; see, e.g., [10, 18] for analogous bounds for stationary (scalar) second order elliptic problems. Optimal error estimates with respect to the polynomial approximation degree can be shown either using the projector of [9] provided the solution belongs to a suitable augmented space, or whenever a continuous interpolant can be built; cf. [26].

3.2 Error estimates in the L^2 norm

In this section we present *a priori* error estimates in the L^2 norm. We follow the approach of [6] for second order hyperbolic equations, and introduce, for a regular enough vector-valued function \mathbf{w} , the elliptic-projection operator $\Pi\mathbf{w}$ defined as

$$\mathcal{A}(\Pi\mathbf{w}, \mathbf{v}) = \mathcal{A}(\mathbf{w}, \mathbf{v}) \quad \forall \mathbf{v} \in \mathbf{V}_{hp}. \quad (19)$$

We immediately have

$$\|\mathbf{u} - \Pi\mathbf{u}\|_{\text{DG}} \leq \|\mathbf{u} - \Pi_{hp}\mathbf{u}\|_{\text{DG}} + \|\Pi_{hp}\mathbf{u} - \Pi\mathbf{u}\|_{\text{DG}} \lesssim \|\Pi_{hp}\mathbf{u} - \mathbf{u}\|_{\text{DG}}, \quad (20)$$

where Π_{hp} is the interpolant of Lemma 3.1, and where the second step follows from Lemma 1.2 and the definition (19)

$$\begin{aligned} \|\Pi_{hp}\mathbf{u} - \Pi\mathbf{u}\|_{\text{DG}}^2 &\lesssim \mathcal{A}(\Pi_{hp}\mathbf{u} - \Pi\mathbf{u}, \Pi_{hp}\mathbf{u} - \Pi\mathbf{u}) = \mathcal{A}(\Pi_{hp}\mathbf{u} - \mathbf{u}, \Pi_{hp}\mathbf{u} - \Pi\mathbf{u}) \\ &\lesssim \|\Pi_{hp}\mathbf{u} - \mathbf{u}\|_{\text{DG}} \|\Pi_{hp}\mathbf{u} - \Pi\mathbf{u}\|_{\text{DG}}. \end{aligned}$$

We also recall the following Poincaré–Friedrichs inequality valid for piecewise vector-valued H^1 functions

$$\|\mathbf{v}\|_{L^2(\mathcal{T}_h)}^2 \lesssim \sum_{K \in \mathcal{T}_h} \|\nabla \mathbf{v}\|_{L^2(K)}^2 + \sum_{F \in \mathcal{F}_h} \frac{1}{h_F} \|[[\mathbf{v}]]\|_{L^2(F)}^2 \quad \forall \mathbf{v} \in [H^1(\mathcal{T}_h)]^d,$$

cf. [5]. Using that $\sum_{K \in \mathcal{T}_h} \|\nabla \mathbf{v}\|_{L^2(K)} \leq \|\varepsilon(\mathbf{v})\|_{L^2(\mathcal{T}_h)}$, and from the definition of the DG norm and of the stabilization function (9), it immediately follows

$$\|\mathbf{v}\|_{L^2(\mathcal{T}_h)}^2 \lesssim \|\mathbf{v}\|_{\text{DG}} \quad \forall \mathbf{v} \in [H^1(\mathcal{T}_h)]^d, \quad (21)$$

Theorem 3.4. (*A-priori error estimate in the L^2 norm.*) Under the Assumptions of Theorem 3.2, it holds

$$\begin{aligned} \sup_{t \in (0, T]} \|\mathbf{e}(t)\|_{L^2(\Omega)}^2 &\lesssim \sup_{t \in (0, T]} \left\{ \frac{h^{2\min(s, p+1)}}{p^{2s-2}} \left(\|\mathbf{u}_t(t)\|_{H^s(\Omega)}^2 + \|\mathbf{u}(t)\|_{H^s(\Omega)}^2 \right) \right\} \\ &+ \int_0^T \left\{ \frac{h^{2\min(s, p+1)}}{p^{2s-2}} \left(\|\mathbf{u}_{tt}(\tau)\|_{H^s(\Omega)}^2 + \|\mathbf{u}_t(\tau)\|_{H^s(\Omega)}^2 \right) \right\} d\tau. \end{aligned}$$

with $h = \max_{K \in \mathcal{T}_h} h_K$, $p = \min_{K \in \mathcal{T}_h} p_K$ and $s = \min_{K \in \mathcal{T}_h} s_K$.

Proof. As in the proof of Theorem 3.2 we decompose the error as $\mathbf{e} = \mathbf{e}^\pi - \mathbf{e}^h$, where now $\mathbf{e}^\pi = \mathbf{u}^h - \Pi\mathbf{u}$ and $\mathbf{e}^h = \mathbf{u} - \Pi\mathbf{u}$, $\Pi\mathbf{u}$ being the elliptic projector defined in (19). With the above decomposition, the error equation (14) becomes:

$$(\rho \mathbf{e}_{tt}^h, \mathbf{v})_{\mathcal{T}_h} + \mathcal{A}(\mathbf{e}^h, \mathbf{v}) = (\rho \mathbf{e}_{tt}^\pi, \mathbf{v})_{\mathcal{T}_h} \quad \forall \mathbf{v} \in \mathbf{V}_{hp}.$$

By taking $\mathbf{v} = \mathbf{e}^h$ in the above identity and reasoning as in the proof of Theorem 2.2, we have

$$\|\mathbf{e}^h\|_{\mathbb{E}}^2 - 2\langle [[\mathbf{e}^h]], \{\mathcal{D}\varepsilon(\mathbf{e}^h)\}_\delta \rangle_{\mathcal{F}_h} \gtrsim \|\mathbf{e}^h\|_{\mathbb{E}}^2,$$

provided that the penalty parameter α is chosen large enough; cf. (6). Therefore, integrating in time between 0 and t and using that $\mathbf{e}^h(0) = \mathbf{u}^h(0) - \mathbf{u}^\pi(0) = \mathbf{0}$, we get

$$\|\mathbf{e}^h\|_{\mathbb{E}}^2 \lesssim \int_0^t (\rho \mathbf{e}_{tt}^\pi, \mathbf{e}_t^h)_{\mathcal{T}_h} d\tau \lesssim \int_0^t \|\mathbf{e}_{tt}^\pi\|_{L^2(\Omega)} \|\mathbf{e}^h\|_{\mathbb{E}} d\tau \quad (22)$$

where the second step follows based on employing the Cauchy-Schwarz inequality. Applying Gronwall's Lemma 2.1 we get

$$\|\mathbf{e}^h(t)\|_{\mathbb{E}} \lesssim \int_0^t \|\mathbf{e}_{tt}^\pi(\tau)\|_{L^2(\Omega)} d\tau \quad \forall t \in (0, T].$$

Next, from the Cauchy-Schwarz inequality, the above bound and the Poincaré–Friedrichs inequality (21), we immediately get

$$\begin{aligned} \|\mathbf{u} - \mathbf{u}^h\|_{L^2(\mathcal{T}_h)} &\lesssim \|\mathbf{e}^\pi\|_{L^2(\mathcal{T}_h)} + \|\mathbf{e}^h\|_{L^2(\mathcal{T}_h)} \lesssim \|\mathbf{e}^\pi\|_{L^2(\mathcal{T}_h)} + \|\mathbf{e}^h\|_{\text{DG}} \\ &\leq \|\mathbf{e}^\pi\|_{L^2(\mathcal{T}_h)} + \|\mathbf{e}^h\|_{\mathbb{E}} \lesssim \|\mathbf{e}^\pi\|_{L^2(\mathcal{T}_h)} + \int_0^t \|\mathbf{e}_{tt}^\pi(\tau)\|_{L^2(\Omega)} d\tau. \end{aligned}$$

The estimate of the terms on the right hand side is based on employing a duality argument; cf [6]. Let $\boldsymbol{\xi}$ be the solution of the problem

$$\nabla \cdot \sigma(\boldsymbol{\xi}) = \mathbf{e}^\pi \quad \text{in } \Omega, \quad \boldsymbol{\xi} = \mathbf{0} \quad \text{on } \partial\Omega.$$

As Ω is convex, the above problem is well-posed and its unique solution $\boldsymbol{\xi} \in [H^2(\Omega)]^d$ and satisfies $\|\boldsymbol{\xi}\|_{H^2(\Omega)} \lesssim \|\mathbf{e}^\pi\|_{L^2(\Omega)}$. Moreover, it holds

$$\|\mathbf{e}^\pi\|_{L^2(\Omega)}^2 = (\mathbf{e}^\pi, \mathbf{e}^\pi)_{L^2(\Omega)} = \mathcal{A}(\boldsymbol{\xi}, \mathbf{e}^\pi) = \mathcal{A}(\boldsymbol{\xi} - \boldsymbol{\xi}^\pi, \mathbf{e}^\pi) \lesssim \|\boldsymbol{\xi} - \boldsymbol{\xi}^\pi\|_{\text{DG}} \|\mathbf{e}^\pi\|_{\text{DG}}$$

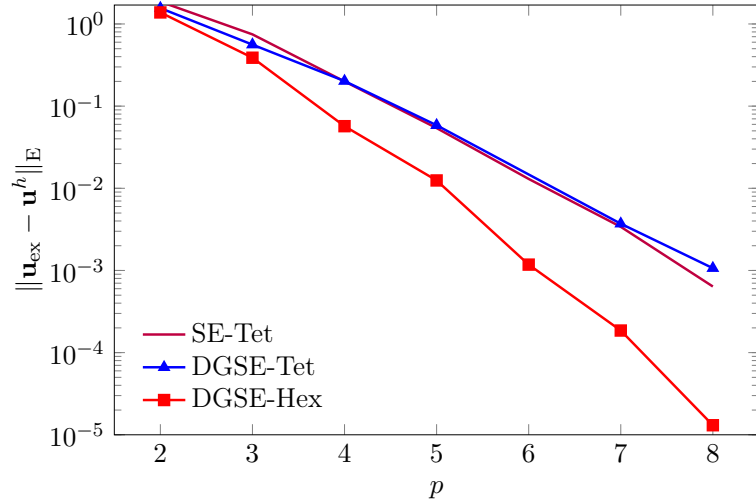
where $\boldsymbol{\xi}^\pi \in \mathbf{V}_{hp}$ is the interpolant of Lemma 3.1, and where the last steps follows from Lemma 1.2. Employing the interpolation estimates of Lemma 3.1 we have

$$\|\mathbf{e}^\pi\|_{L^2(\Omega)}^2 \lesssim \frac{h}{p^{1/2}} \|\boldsymbol{\xi}\|_{H^2(\Omega)} \|\mathbf{e}^\pi\|_{\text{DG}} \lesssim \frac{h}{p^{1/2}} \|\mathbf{e}^\pi\|_{L^2(\Omega)} \|\mathbf{e}^\pi\|_{\text{DG}},$$

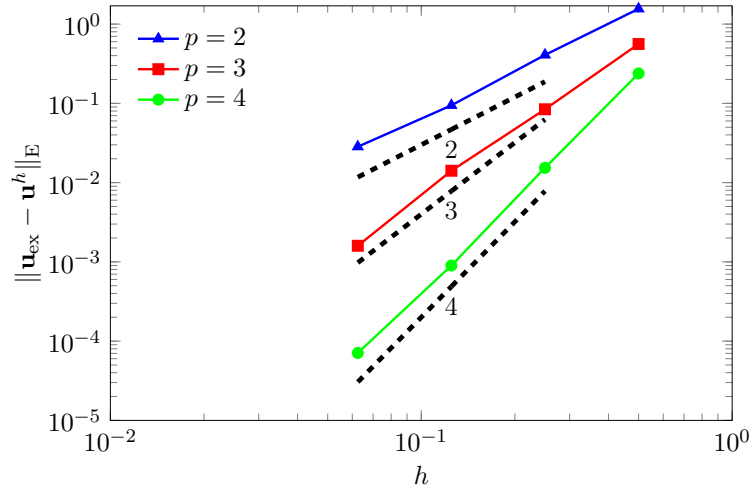
where $h = \max_{K \in \mathcal{T}_h} h_K$ and $p = \min_{K \in \mathcal{T}_h} p_K$. The proof is completed by employing the error bounds of Theorem 3.2. \square

4 Numerical results

The results of this section have been obtained with *SPEED* (<http://speed.mox.polimi.it/>), an open source Fortran code developed at Politecnico di Milano by the Laboratory for Modeling and Scientific Computing MOX of the Department of Mathematics and the Department of Civil and Environmental Engineering. *SPEED* is specifically designed for the simulation of seismic waves propagation problems, including both the ground motion induced by large scale earthquakes and soil-structure interaction in urban areas; see, e.g., [16]. Throughout the section we have set the time step $\Delta t = 10^{-5}$ so that



(a) Computed errors versus p .



(b) Computed errors versus h .

Figure 1: Example 1. Fig.1(a): computed errors measured in the energy norm $\|\cdot\|_E$ at $t = T = 0.05$ versus the polynomial degree p for a tetrahedral mesh (DG-Tet) and a hexahedral grid (DG-Hex). The results are also compared with the corresponding one based on employing conforming Spectral Element on the same tetrahedral grid (SE-Tet). Fig. 1(b): computed errors measured in the energy norm $\|\cdot\|_E$ at $t = T$ versus the mesh size for $p = 2, 3, 4$. The dashed lines denote the expected slopes of the error curves.

the temporal component of the error is negligible compared to the spatial one.

In the first example we consider an elastic wave propagation problem in $\Omega = (0, 1)^3$, with $\rho = \lambda = \mu = 1$. The source term \mathbf{f} and the initial data are chosen so that the exact solution of problem (1) is given by

$$\mathbf{u}_{\text{ex}}(x, y, z, t) = \sin(3\pi t) \begin{bmatrix} -\sin^2(\pi x) \sin(2\pi y) \sin(2\pi z) \\ \sin^2(\pi y) \sin(2\pi x) \sin(2\pi z) \\ \sin^2(\pi z) \sin(2\pi x) \sin(2\pi y) \end{bmatrix}.$$

We first we consider both a tetrahedral and a hexahedral grid with mesh size $h = 0.5$ and let the polynomial degree p vary from 2 to 8. In Figure 1(a) we report the error computed in the energy norm $\|\cdot\|_{\text{E}}$ at $t = T = 0.05$ and as a function of the polynomial degree. As expected, an exponential convergence is observed. For the sake of comparison Figure 1(a) also reports the corresponding computed errors obtained with a conforming Spectral Element method on the the same tetrahedral grid. Next, we investigate the behaviour of the error as a function of the grid size h for different polynomial degrees. We consider a sequence of uniformly refined tetrahedral grids starting from an initial decomposition of size $h_0 = 0.5$. In Figure 1(b) we report the computed errors measured in energy norm $\|\cdot\|_{\text{E}}$ at the final observation time $t = T$ versus the grid size for $p = 2, 3, 4$. As expected, the results confirm a convergence rate of order p .

In the second test we consider a plane wave propagating along the vertical direction in a layered elastic half-space $\Omega = (0, 100) \times (0, 100) \times (-300, 0) \text{ m}$, see Figure 2 (left). In Table ?? we report the depth

Layer	Depth [m]	ρ [Kg/m ³]	c_P [m/s]	c_S [m/s]	Dumping ξ [1/s]
Ω_1	200	2200	4000	2000	$\pi \times 10^{-3}$
Ω_2	100	1800	600	300	$\pi \times 10^{-2}$

Table 1: Example 2. Material properties.

and the material properties of the half-space Ω_1 and the layer Ω_2 . The source plane wave is polarized in the x direction and its time dependency is given by a unit amplitude Ricker wave with peak frequency at 1 Hz. A damping term proportional to $2\rho\xi\mathbf{u}_t + 2\xi^2\mathbf{u}$, with ξ as in Table ??, is also added to the equation to take into account viscoelastic effects. The subdomains Ω_1 and Ω_2 are discretized with a hexahedral and tetrahedral meshes, respectively, and the computational grids are built in order to have at least five grid points per wavelength, with a polynomial degree equal to 4 in both Ω_1 and Ω_2 . Finally, we impose absorbing boundary conditions on the bottom surface, a free surface condition on the top surface, and homogeneous Dirichlet conditions for the y and z component of the displacement on the remaining boundaries. In Figure 2 (right) we report the computed solution which is

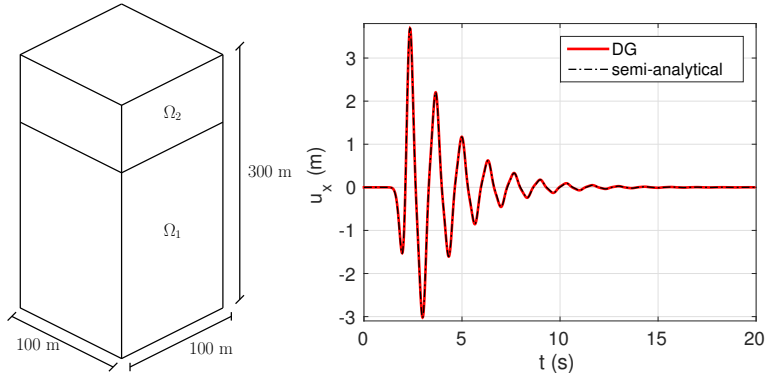


Figure 2: Example 2. Left: Computational domain $\Omega = \Omega_1 \cup \Omega_2$. The elastic wave propagates from the bottom of Ω_1 to the top surface of Ω_2 . Right: Computed time history of the x component of the displacement \mathbf{u}_x recorded at $R = (50, 50, 0) m$. The results are compared with a reference semi-analytical solution \mathbf{u}_{TH} obtained with the Thomson-Haskell propagation matrix method.

also compared with a reference semi-analytical solution \mathbf{u}_{TH} based on the Thomson-Haskell propagation matrix method. More precisely, Figure 2 (right) shows the time history of the x component of the displacement \mathbf{u}_x recorded at the point $R = (50, 50, 0) m$. Finally, in Figure 3 we report four snapshots of the deformed computational domain when invested by the plane wave. Two relevant physical effects can be observed: *i*) the wave field is amplified at the top of the domain due to the free surface condition; *ii*) reflections of the wave field take place inside the layer Ω_2 characterized by a softer material with respect to the half space Ω_1 .

References

- [1] P. F. Antonietti, B. Ayuso de Dios, I. Mazzieri, and A. Quarteroni. Stability analysis of discontinuous Galerkin approximations to the elastodynamics problem. *J. Sci. Comput.*, 68(1):143–170, 2016.
- [2] D. N. Arnold. An interior penalty finite element method with discontinuous elements. *SIAM J. Numer. Anal.*, 19(4):742–760, 1982.
- [3] D. N. Arnold, F. Brezzi, B. Cockburn, and L. D. Marini. Unified analysis of discontinuous Galerkin methods for elliptic problems. *SIAM J. Numer. Anal.*, 39(5):1749–1779, 2001/02.
- [4] D. N. Arnold, F. Brezzi, R. S. Falk, and L. D. Marini. Locking-free Reissner-Mindlin elements without reduced integration. *Comput. Methods Appl. Mech. Engrg.*, 196(37-40):3660–3671, 2007.
- [5] S. C. Brenner. Korn’s inequalities for piecewise H^1 vector fields. *Math. Comp.*, 73(247):1067–1087, 2004.

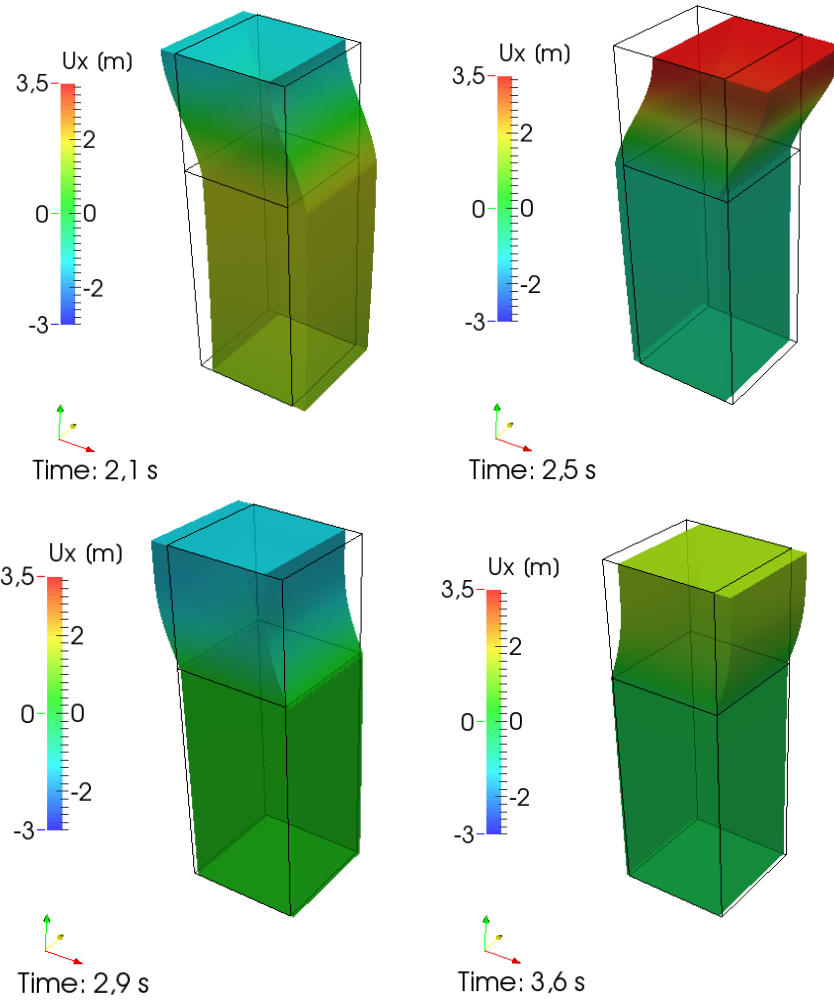


Figure 3: Example 2. Snapshots of the x -component of the displacement \mathbf{u}_x . The deformed domain (coloured) is compared with the non distorted one (black line).

- [6] T. Dupont. L^2 -estimates for Galerkin methods for second order hyperbolic equations. *SIAM J. Numer. Anal.*, 10:880–889, 1973.
- [7] E. Faccioli, F. Maggio, R. Paolucci, and A. Quarteroni. 2d and 3d elastic wave propagation by a pseudo-spectral domain decomposition method. *Journal of Seismology*, 1(3):237–251, 1997.
- [8] E. H. Georgoulis, E. Hall, and P. Houston. Discontinuous Galerkin methods for advection-diffusion-reaction problems on anisotropically refined meshes. *SIAM J. Sci. Comput.*, 30(1):246–271, 2007/08.
- [9] E. H. Georgoulis and E. Süli. Optimal error estimates for the hp -version interior penalty discontinuous Galerkin finite element method. *IMA J. Numer. Anal.*, 25(1):205–220, 2005.
- [10] P. Houston, C. Schwab, and E. Süli. Discontinuous hp -finite element methods for advection-diffusion-reaction problems. *SIAM J. Numer. Anal.*, 39(6):2133–2163, 2002.
- [11] D. Komatitsch, J. Ritsema, and J. Tromp. Geophysics: The spectral-element method, beowulf computing, and global seismology. *Science*, 298(5599):1737–1742, 2002.
- [12] D. Komatitsch and J. Tromp. Introduction to the spectral element method for three-dimensional seismic wave propagation. *Geophysical Journal International*, 139(3):806–822, 1999.
- [13] D. Komatitsch and J. Tromp. Spectral-element simulations of global seismic wave propagation - i. validation. *Geophysical Journal International*, 149(2):390–412, 2002.
- [14] D. Komatitsch, J.-P. Vilotte, R. Vai, J. Castillo-Covarrubias, and F. Sánchez-Sesma. The spectral element method for elastic wave equations - application to 2-d and 3-d seismic problems. *International Journal for Numerical Methods in Engineering*, 45(9):1139–1164, 1999.
- [15] D. J. P. Lahaye, F. Maggio, and A. Quarteroni. Hybrid finite element–spectral element approximation of wave propagation problems. *East-West J. Numer. Math.*, 5(4):265–289, 1997.
- [16] I. Mazzieri, M. Stupazzini, R. Guidotti, and C. Smerzini. SPEED: SPectral Elements in Elastodynamics with Discontinuous Galerkin: a non-conforming approach for 3D multi-scale problems. *Internat. J. Numer. Methods Engrg.*, 95(12):991–1010, 2013.
- [17] A. T. Patera. Spectral methods for spatially evolving hydrodynamic flows. In *Spectral methods for partial differential equations (Hampton, Va., 1982)*, pages 239–256. SIAM, Philadelphia, PA, 1984.
- [18] I. Perugia and D. Schötzau. An hp -analysis of the local discontinuous Galerkin method for diffusion problems. *J. Sci. Comput.*, 17(1-4):561–571, 2002.
- [19] A. Quarteroni. *Numerical models for differential problems*, volume 8 of *MS&A. Modeling, Simulation and Applications*. Springer, Milan, second edition, 2014. Translated from the fifth (2012) Italian edition by Silvia Quarteroni.

- [20] B. Rivière, S. Shaw, M. F. Wheeler, and J. R. Whiteman. Discontinuous Galerkin finite element methods for linear elasticity and quasistatic linear viscoelasticity. *Numer. Math.*, 95(2):347–376, 2003.
- [21] B. Rivière, S. Shaw, and J. R. Whiteman. Discontinuous Galerkin finite element methods for dynamic linear solid viscoelasticity problems. *Numer. Methods Partial Differential Equations*, 23(5):1149–1166, 2007.
- [22] B. Rivière and M. F. Wheeler. Discontinuous finite element methods for acoustic and elastic wave problems. In *Current trends in scientific computing (Xi'an, 2002)*, volume 329 of *Contemp. Math.*, pages 271–282. Amer. Math. Soc., Providence, RI, 2003.
- [23] C. Schwab. *p- and hp-finite element methods*. Numerical Mathematics and Scientific Computation. The Clarendon Press, Oxford University Press, New York, 1998. Theory and applications in solid and fluid mechanics.
- [24] G. Seriani, E. Priolo, and A. Pregarz. Modelling waves in anisotropic media by a spectral element method. In *Mathematical and numerical aspects of wave propagation (Mandelieu-La Napoule, 1995)*, pages 289–298. SIAM, Philadelphia, PA, 1995.
- [25] C. Smerzini, R. Paolucci, and M. Stupazzini. Experimental and numerical results on earthquake-induced rotational ground motions. *Journal of Earthquake Engineering*, 13(1 SUPPL. 1):66–82, 2009.
- [26] B. Stamm and T. P. Wihler. *hp*-optimal discontinuous Galerkin methods for linear elliptic problems. *Math. Comp.*, 79(272):2117–2133, 2010.
- [27] R. Stenberg. Mortaring by a method of J. A. Nitsche. In *Computational mechanics (Buenos Aires, 1998)*. Centro Internac. Métodos Numér. Ing., Barcelona, 1998.
- [28] M. Stupazzini, R. Paolucci, and H. Igel. Near-fault earthquake ground-motion simulation in the grenoble valley by a high-performance spectral element code. *Bulletin of the Seismological Society of America*, 99(1):286–301, 2009.
- [29] M. F. Wheeler. An elliptic collocation-finite element method with interior penalties. *SIAM J. Numer. Anal.*, 15(1):152–161, 1978.

MOX Technical Reports, last issues

Dipartimento di Matematica
Politecnico di Milano, Via Bonardi 9 - 20133 Milano (Italy)

- 32/2016** Tarabelloni, N.; Schenone, E.; Collin, A.; Ieva, F.; Paganoni, A.M.; Gerbeau, J.-F.
Statistical Assessment and Calibration of Numerical ECG Models
- 30/2016** Abramowicz, K.; Häger, C.; Pini, A.; Schelin, L.; Sjöstedt de Luna, S.; Vantini, S.
Nonparametric inference for functional-on-scalar linear models applied to knee kinematic hop data after injury of the anterior cruciate ligament
- 31/2016** Antonietti, P.F.; Merlet, B.; Morgan, P.; Verani, M.
Convergence to equilibrium for a second-order time semi-discretization of the Cahn-Hilliard equation
- 28/2016** Antonietti, P.F.; Dal Santo, N.; Mazzieri, I.; Quarteroni, A.
A high-order discontinuous Galerkin approximation to ordinary differential equations with applications to elastodynamics
- 29/2016** Miglio, E.; Parolini, N.; Penati, M.; Porcù, R.
GPU parallelization of brownout simulations with a non-interacting particles dynamic model
- 27/2016** Repposi, E.; Rosso, R.; Verani, M.
A phase-field model for liquid-gas mixtures: mathematical modelling and Discontinuous Galerkin discretization
- 26/2016** Brunetto, D.; Calderoni, F.; Piccardi, C.
Communities in criminal networks: A case study
- 25/2016** Baroli, D.; Cova, C.M.; Perotto, S.; Sala, L.; Veneziani, A.
Hi-POD solution of parametrized fluid dynamics problems: preliminary results
- 24/2016** Pagani, S.; Manzoni, A.; Quarteroni, A.
A Reduced Basis Ensemble Kalman Filter for State/parameter Identification in Large-scale Nonlinear Dynamical Systems
- 23/2016** Fedele, M.; Faggiano, E.; Dedè, L.; Quarteroni, A.
A Patient-Specific Aortic Valve Model based on Moving Resistive Immersed Implicit Surfaces